

## REFINEMENT OF Al-5%Cu AND Al-25%Cu ALLOYS BY MEANS OF KOBO METHODS

This study was undertaken to investigate the effect of severe plastic deformation (SPD) by extrusion combined with reversible torsion (KoBo) method on microstructure and mechanical properties of Al-5Cu and Al-25Cu alloys. The extrusion combined with reversible torsion was carried out using reduction coefficient of  $\lambda = 30$  and  $\lambda = 98$ . In this work, the microstructure was characterized by light microscopy (LM), scanning electron microscopy (SEM) and scanning transmission electron microscopy (STEM). Compression test and tensile test were performed for deformed alloys. The binary Al-5Cu and Al-25Cu alloys consist of the face centered cubic (FCC)  $\alpha$  phase in the form of dendrites and tetragonal (C16)  $\theta$ -Al<sub>2</sub>Cu intermetallic phase observed in interdendritic regions. The increase of Cu content leads to increase of interdendritic regions. The microstructure of the alloys is refined after applying KoB deformation with  $\lambda = 30$  and  $\lambda = 98$ . Ultimate Tensile Strength (UTS) of Al-5Cu alloy after KoBo deformation with  $\lambda = 30$  and  $\lambda = 98$  reached about 200 MPa. UTS for samples of Al-25Cu with  $\lambda = 30$  and  $\lambda = 98$  increased compared to Al-5Cu alloy and exceed 320 MPa and 270 MPa respectively. All samples showed increase of plasticity with increase of reduction coefficient. Independently of reduction coefficient, the compressive strain of Al-5Cu alloys is about 60%. The Al-25Cu alloy with  $\lambda = 98$  showed the value of compressive strain exceed 60%, although for this same alloy but with  $\lambda = 30$ , the compressive strain is only 35%.

*Keywords:* Al-Cu alloys, severe plastic deformation, ultrafine-grains, microstructure, STEM

## 1. Introduction

The strengthened Al-Cu alloys are commonly used for structural engineering applications, and in civil engineering [1-3]. The precipitation hardened alloys (for example series 2xxx) are commonly processed by extrusion and are characterized by good strength properties and high elastically module. Al-Cu alloys above 5% Cu are known as cast alloys and are not plastic deformable. These as-cast alloys, depending on alloy composition (Cu content for bimodal composition) and solidification conditions contain an Al matrix with a wide range of intermetallic phases. The intermetallic phases are responsible especially for formability, mechanical properties and fracture behavior of Al-Cu alloys. From practical point of view, increase of intermetallic phase in alloy may increase mechanical properties and use of these alloys at higher temperatures [3,4]. Although its fracture toughness and formability decreases [3,5]. Deformation of as-cast alloys is possible thanks to severe plastic deformation methods (SPD) methods. Extrusion combined with reversible torsion (KoBo) (Fig. 1) is one of such SPD method [6,7]. Due to the complex state of stress and deformation enables

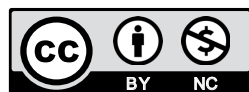
deformation practically non deformable materials. Under conditions induced by KoBo, when the process is realized with higher deformation intensity it is possible to obtain the higher strength properties. Additionally temperature of deformed material can rise enough to generate some structural changes indicating the occurrence of dynamic recovery and recrystallization [6], in consequence, the observed structure becomes composed very often of equiaxed grains, which are typical for increase of plastically properties.

As mentioned previously, in as-cast Al-Cu alloys the most typical is intermetallic phase as Al<sub>2</sub>Cu [8-12], this phase in dependent of chemical composition are arranged in interdendritic channels of  $\alpha$  matrix. The brittle, tetragonal (C16)  $\theta$ -Al<sub>2</sub>Cu phase, operate as nucleation sites for cracks and broke by transcrystalline cleavage mechanism. Data in the literature [3,5] shows that damage during extrusion begins by decohesion process along Al<sub>2</sub>Cu interfaces. The Al<sub>2</sub>Cu intermetallic phase can act as crack initiation because difference in crystal structure and large stress concentrations can be introduced during deformation, thereby reducing the ductility. For this reason mechanical properties, especially ductility performed in room temperature of these

<sup>1</sup> SILESIAŃ UNIVERSITY OF TECHNOLOGY, FACULTY OF MATERIALS ENGINEERING, 8 KRASIŃSKIEGO STR., 40-019 KATOWICE, POLAND

<sup>2</sup> INSTITUTE OF NON-FERROUS METALS, 5 SOWIŃSKIEGO STR., 44-100 GLIWICE, POLAND

\* Corresponding author: kinga.rodak@polsl.pl



materials may be insufficient. SPD processes can introduce into the deformed structure non equilibrium grain boundary nature, and can as mentioned above, introduce processes connected with reconstruction of deformed structure as recovery and recrystallization [3,13,14]. Hence, these elements may affect the resistance to fracture. Moreover the resistance to fracture and damage may be strongly influenced by the shape, distribution and volume fraction of the second phase particles. It is well known, that SPD processes give possibility to change the size and morphology of deformed intermetallic phases. A literature review on Al-Cu alloys indicates that research work on the SPD deformed alloy with comparable chemical composition have not been attempted, except a few works [8,10].

This study aimed to obtain ultrafine two-phase microstructures of an Al-Cu alloy by KoBo processing. The application of SPD to the grain refinement in Al-5Cu and Al-25Cu is extremely difficult because the two phase microstructure with a high volume fraction of the secondary phase is not ductile enough to tolerance severe plastic deformation. Thus, in this article the structural and mechanical properties of grain refinement of Al-Cu alloy with a high volume fraction of Al<sub>2</sub>Cu phase using the KoBo method has been presented.

## 2. Experiments

The material for KoBo deformation was Al-Cu alloy with 5% wt. of Cu (Al-5Cu) and with 25% wt. of Cu (Al-25Cu). The materials were obtained by melting in the Leybold-Heraeus furnace. The materials were melted in graphite crucible. The melted alloys were cast into a round moulds with a diameter of 50 mm, and allowed to cool down. After cooling, the ingots were removed from the moulds. They were machining to 49.5 mm in diameter and were cut to the length of 100 mm. The SPD processing was carried out with the modernized KoBo 2.5 MN horizontal hydraulic press. The recipient temperature was about 130°C. All tests were carried out at constant angle die rotation, which was 8°. The die rotation frequency was 5 Hz. KoBo processing was performed to the 9 mm diameter ( $\varphi$  9) of rods with reduction coefficient ( $\lambda = 30$ ) and to the 5 mm diameter ( $\varphi$  5) of rods with reduction coefficient ( $\lambda = 98$ ).

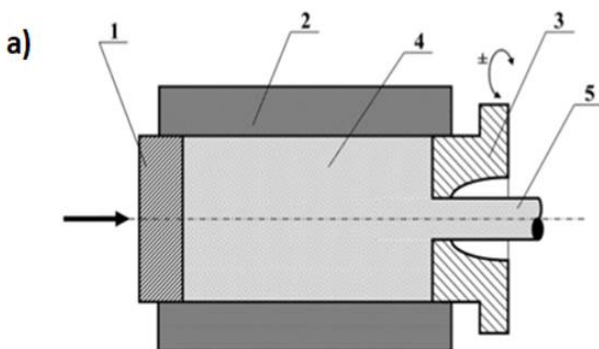


Fig. 1. Schematic illustration of KoBo device: 1 – punch, 2 – container, 3 – periodically rotated die with grooves on face, 4 – extruded metal, 5 – product [6]

The reduction coefficient  $\lambda$  is expressed as follows Eq. (1):

$$\lambda = \frac{d_0^2}{d_k^2} \quad (1)$$

$d_0$  – diameter of extruded ingot,  $d_k$  – rod diameter after KoBo.

The microstructure has been analyzed by optical microscope Olympus GX71, scanning electron microscope ZEISS LEO GEMINI 1525 and scanning transmission electron microscope (STEM) Hitachi HD-2300A equipped with FEG gun. The compression tests were performed on a Zwick / Roell Z100 machine at room temperature on cylindrical shaped samples with the dimension of 6 mm in diameter and 9 mm in high. 100 kN pressure force was applied. Three compression tests were performed on each sample and the average values were calculated. The tensile tests were performed on a Zwick / Roell Z050 machine at room temperature at the initial strain rate of  $2 \times 10^{-3} \text{ s}^{-1}$ . Three tensile tests were performed on each sample and the average values were calculated. The dimensions of the samples were: diameter  $d_o = 4 \text{ mm}$ , length  $l_o = 50 \text{ mm}$ .

## 3. Results and discussion

In initial state (as-cast state) of Al-5Cu alloy (Fig. 2a) and Al-25Cu alloy (Fig. 2b) the dendrites of  $\alpha$  phase (white field in LM microstructure) were observed. The alloys contain a wide range of various intermetallic particles in size. Generally, in

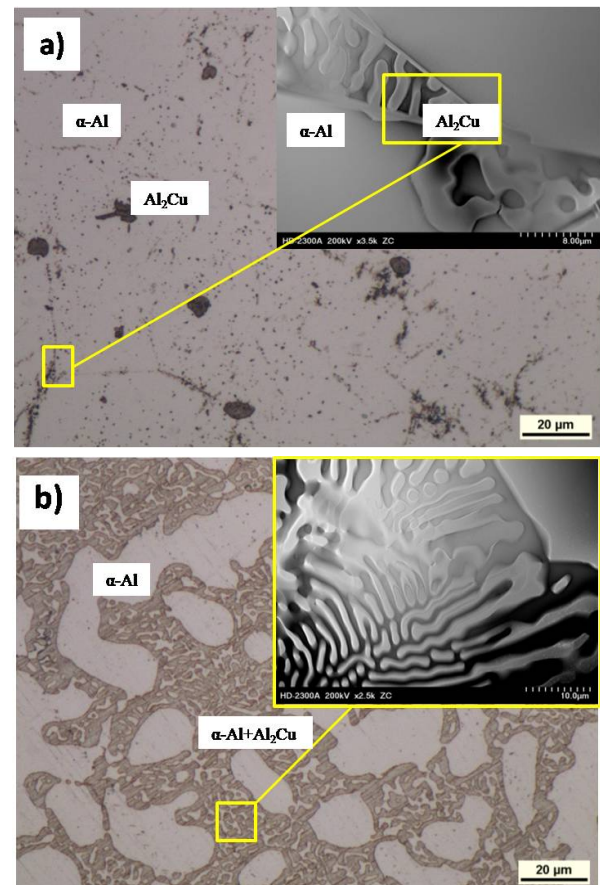


Fig. 2. a) As cast state of Al-5Cu alloy (a) and Al-25Cu alloy (b)

microstructure of Al-5Cu alloy, two populations of intermetallic particles are visible as large particles with eutectic composition and dispersoids. The interdendritic regions of Al-25Cu alloy consisted of massive eutectoid composition ( $\alpha + \text{Al}_2\text{Cu}$  phase) (Fig. 2b). It is evident, that increase of Cu content leads to increase of interdendritic regions (compare Fig. 2a and 2b). Microstructure investigations using STEM (Z contrast) (upper right corners in Fig. 2a,b) enable identification of micrometric lamellar structure of the  $\theta\text{-Al}_2\text{Cu}$  phase and the  $\alpha\text{-Al}$  matrix.

The Al-5Cu alloy after KoBo processing contains intermetallic particles (white area) distributed randomly in the  $\alpha\text{-Al}$  matrix (Fig. 3). The STEM analysis showed two types of  $\text{Al}_2\text{Cu}$  particles: a small spherical and an irregular shaped particles. It is difficult to say what massive regions of eutectoid composition in Al-5Cu alloy is deformed compared with initial. Increase of deformation (increase of  $\lambda$ ) not introduce noticeable changes in microstructure. However, a characteristic fibrous structure can be seen in the longitudinal section (Fig. 3a,c) as a results of extrusion process. Investigations using STEM technique showed that refinement of the  $\alpha\text{-Al}$  matrix as a result of the KoBo deformation can occurred. The diameter of refined grains is about 1  $\mu\text{m}$ . The microstructure of Al-5Cu alloy after deformation revealed that most of the dislocations, introduced during deformation are presented near the  $\text{Al}_2\text{Cu}$  particles (Fig. 4a). The bigger particles of  $\text{Al}_2\text{Cu}$  phase are visible in grain/subgrain boundaries. No evident difference in microstructure after deformation at  $\lambda = 30$  and  $\lambda = 98$  have been observed. In some microareas the grains/subgrains are near free of dislocations (Fig. 4b,c) but in another areas inside grains/subgrains are visible small  $\text{Al}_2\text{Cu}$  particles which act as effective barriers of dislocation movement (Fig. 4d). Moreover, small  $\text{Al}_2\text{Cu}$  particles are effective in creation of subgrain boundaries (Fig. 4d).

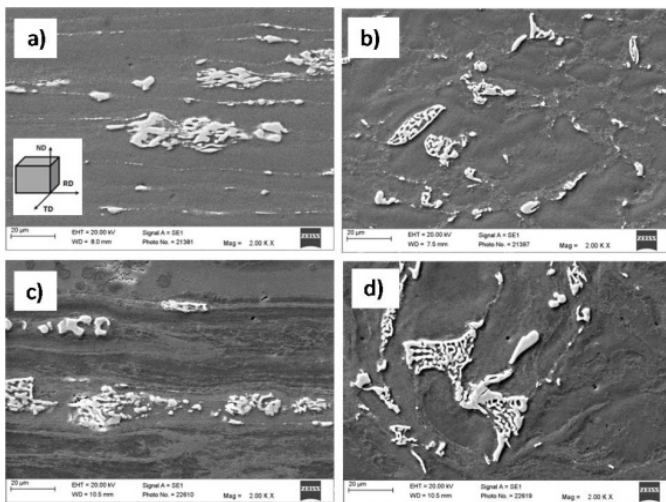


Fig. 3. SEM microstructure in longitudinal and transverse section of Al-5Cu alloy after KoBo processing. Reduction coefficient  $\lambda = 30$  (a,b) and  $\lambda = 98$  (c,d)

In Al-25Cu alloy, deformation process is connected with redistribution of  $\text{Al}_2\text{Cu}$  phase, which assured a more homogeneous microstructure (Fig. 5c,d). The  $\theta\text{-Al}_2\text{Cu}$  phase are characterized by more globular shape compared with as-cast sample (see

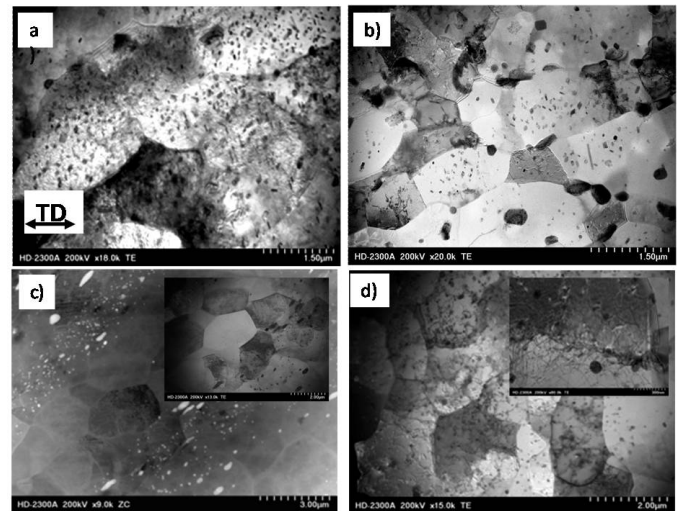


Fig. 4. STEM microstructure of Al-5Cu alloy after KoBo processing. Reduction coefficient  $\lambda = 30$  (a,b) and  $\lambda = 98$  (c,d)

Fig. 2b). Should be note, based on microstructure investigations that structure after KoBo deformation is not completely fragmented. Quite frequently are observed massive microareas of  $\text{Al}_2\text{Cu}$  phase and not fragmented eutectoid composition of  $\text{Al}_2\text{Cu}$  phases. Fibrous structure (Fig. 5a,c) of  $\alpha$  and  $\text{Al}_2\text{Cu}$  phases is evident. Moreover, differences in microstructures obtained with using SEM for  $\lambda = 30$  and for  $\lambda = 98$  are not visible. Detailed investigations using scanning transmission electron microscopy (Fig. 6) showed that, grains of the  $\alpha\text{-Al}$  phase have a higher dislocations density especially in the areas where small particles of  $\text{Al}_2\text{Cu}$  phase were observed (Fig. 6a). In areas of  $\alpha\text{-Al}$  where small particles of  $\text{Al}_2\text{Cu}$  phase are not visible, dislocations density is small. New grains/subgrains created during KoBo deformation are characterized by near equiaxed shape. The role of small and very small particles of  $\text{Al}_2\text{Cu}$  phase is the same as in Al-5Cu alloy. Small particles of  $\text{Al}_2\text{Cu}$  phase are responsible for blocking of grain/subgrain boundaries and dislocation motion.

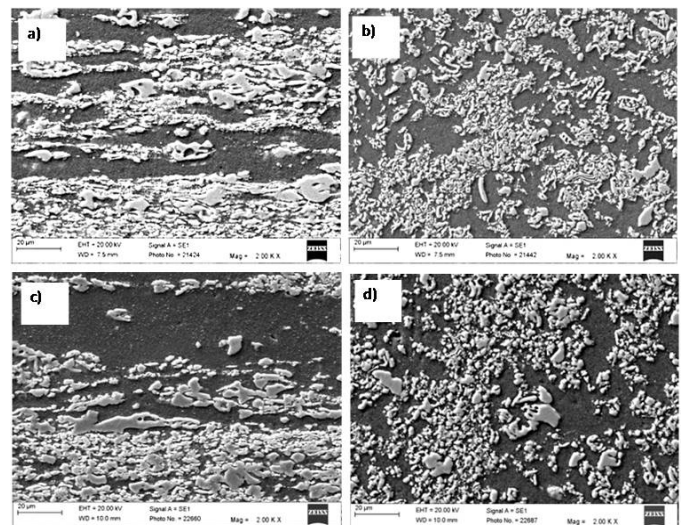


Fig. 5. SEM microstructure in longitudinal and transverse section of Al-25Cu alloy after KoBo processing. Reduction coefficient  $\lambda = 30$  (a,b) and  $\lambda = 98$  (c,d)

Visible on SEM microstructures massive fragments of  $\text{Al}_2\text{Cu}$  phases look like deformed on STEM microstructures (Fig. 6c,d). Based on STEM investigations, it is evident that increase of deformation (increase of  $\lambda$ ) influence on increase of  $\text{Al}_2\text{Cu}$  phase refinement by create many grains/subgrains boundaries. Separated by these boundaries grains/subgrains have dimension smaller than 200 nm (Fig. 6d).

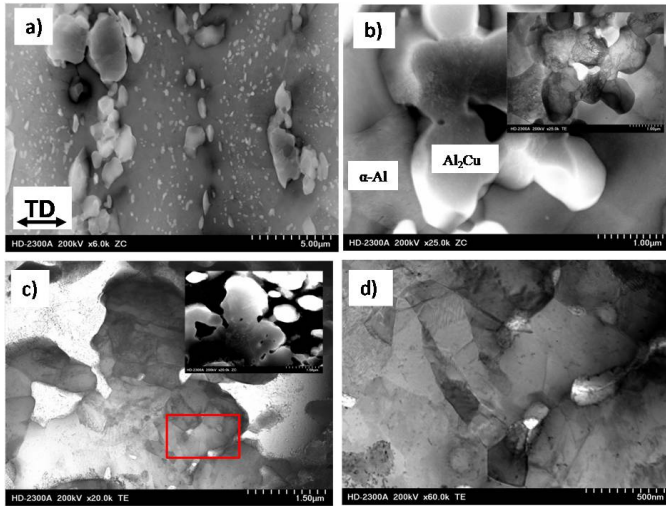


Fig. 6. STEM microstructure of Al-25Cu alloy after KoBo processing. Reduction coefficient  $\lambda = 30$  (a,b) and  $\lambda = 98$  (c,d). Fig. d) is the enlarged area marked with a red square on Fig. c)

The results of mechanical properties measurements are summarized in Table 1.

TABLE 1

Measured mechanical parameters: yield strength ( $YS$ ), ultimate tensile strength ( $UTS$ ), elongation to fracture ( $A_c$ ), compressive strength ( $R_c$ ), compressive strain ( $S_c$ ) of deformed Al-Cu alloys

Alloy/ $\lambda$	( $YS$ ) MPa	( $UTS$ ) MPa	( $A_c$ ) %	( $R_c$ ) MPa	( $S_c$ ) %
Al5Cu (30)	75±6	208±9	46±1	202±3	60±4
Al5Cu (98)	104±8	191±9	55±1	203±5	67±6
Al25Cu (30)	92±5	328±5	12±2	172±7	35±6
Al25Cu (98)	126±9	280±7	13±5	340±7	67±8

The stress-strain results obtained in static compressive test are shown in Fig. 7. Compressive strength ( $R_c$ ) of Al-5Cu alloy for samples with different value of deformation  $\lambda = 30$  and for  $\lambda = 98$  and are near comparable. The value of  $R_c$  exceed 200 MPa. All samples showed a good plasticity, the compressive strain is about 60% and 67% for the alloy deformed with  $\lambda = 30$  and  $\lambda = 98$ .

The compressive strength  $R_c$  of Al-25Cu alloy is noticeably higher compared to the

Al-5Cu alloy but only for higher value of deformation. For Al-25Cu alloy deformed with  $\lambda = 98$  the  $R_c$  is 340 MPa. The Al-25Cu alloy deformed with  $\lambda = 30$  showed lower  $R_c$  (up to 170 MPa), most probably due to the cracks forming after compression tests as was observed (Fig. 7). Generally, should be noted, that compression test realized for Al-25Cu alloy was stopped due to

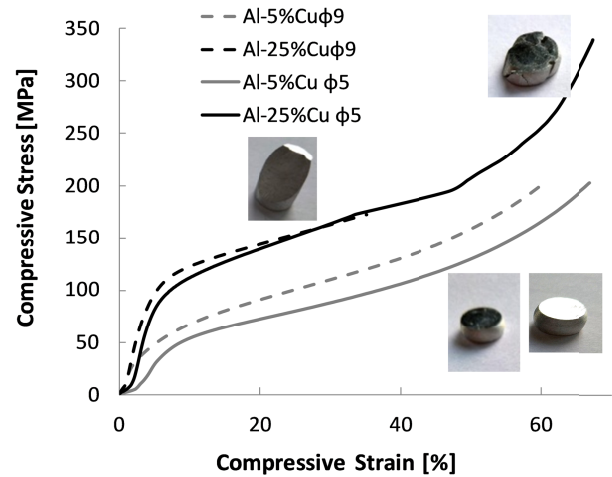


Fig. 7. The static compressive test obtained in for Al-5Cu and Al-25Cu alloy after KoBo processing

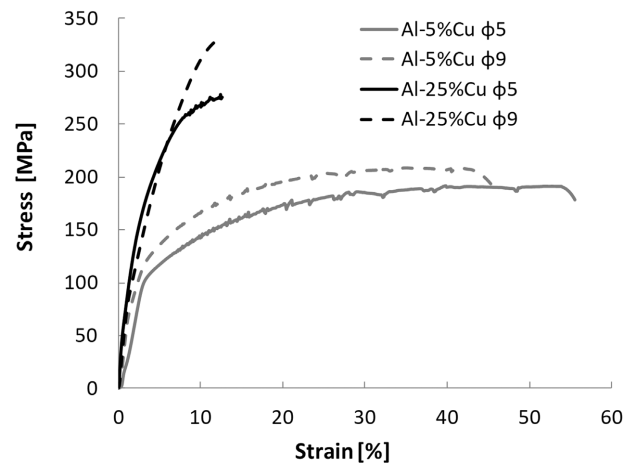


Fig. 8. The stress-strain results obtained in static tensile test for Al-5Cu and Al-25Cu alloy after KoBo processing

sample cracking. Failure of the Al-25Cu alloy with  $\lambda = 30$  was quite suddenly and specimens showed sliding cracks at an angle of approx.  $45^\circ$  to the specimens axis, this is a characteristic feature of brittle materials (Fig. 7). After deformation with  $\lambda = 98$ , the Al-25Cu alloy also failure, but without sliding cracks, for this reason, the value of compressive strain ( $S_c$ ) is about two time higher than for sample deformed with  $\lambda = 30$ .

Fig. 8 shows tensile test curves of the samples after KoBo processing. Ultimate tensile strength (UTS) of Al-5Cu alloy with  $\lambda = 30$  and  $\lambda = 98$  reached 208 MPa and 191 MPa respectively. Increase in deformation lead to decrease in the plasticity. Elongation to fracture ( $A_c$ ) reached 46% and 55% for  $\lambda = 30$  and  $\lambda = 98$  respectively. Deformed Al-25Cu alloys showed high strength. UTS was 328 MPa and 280 MPa for  $\lambda = 30$  and  $\lambda = 98$  respectively. Strengthening by the increase of intermetallic phase in the Al-25Cu alloys was accompanied by a drastic drop of ductility. Elongation to fracture ( $A_c$ ) reached 12% and 13% for  $\lambda = 30$  and  $\lambda = 98$  respectively. It is interesting to note that serrations were seen in the stress-strain curves. Serrated yielding associated with negative strain-rate sensitivity has frequently been observed in

Al alloys during tensile or compression deformation at room temperature [15].

The obtained results leads to the conclusion that increase of deformation by KoBo realized by increase of  $\lambda$  can produce material with higher plastic properties. Higher value of  $\lambda$ , guarantees decrease in UTS and increase in elongation to fracture.

Obtained results for A-5Cu alloy, mean that increase of deformation not influence on strength properties in compression test, but in tensile test a slightly lower strength was observed. Obtained results are confirmed by SEM and STEM results, where microstructures are near comparable. The function of small precipitates is mainly to stop the movement of dislocations and grain boundaries. Should be assumed that in Al-5Cu alloy the processes of recovery in deformed samples with higher value of deformation dominate and makes possibility in higher relative reduction.

The higher strength of Al-25Cu alloy compared with Al-5Cu alloy is caused by the intermetallic phase strengthening. The reason of this may be effective process of massive Al<sub>2</sub>Cu phase refinement. There evolution of Al<sub>2</sub>Cu phase microstructure is associated with creation of dislocation structure, easy redistribution of dislocation structure and creation of ultrafine grains with diameter near similar to ultrafine grain of  $\alpha$ -Al matrix. This situation is connected with the fact that for Al-25Cu alloy, the processes of refinement may can proceed easier than in matrix. The obtained results are in accordance with the literature [8]. During deformation in Al<sub>2</sub>Cu phase is observed mechanism connected with non-conservative motion of glide dislocation. This mechanism provide rapid diffusion channels during plastic deformation and indicates structural instability of intermetallic phase. For this reason the process of dislocations redistribution, including influence of point defects can influence on effective grain refinement of massive Al<sub>2</sub>Cu phase.

There is only limited information in the literature in the theme connected with understanding of the deformation process of the two phase microstructure of Al-Cu alloy with a high volume fraction of secondary phase on mechanical properties.

In [16] ECAP was successfully applied on a lamellae eutectic alloy of Al-33%Cu at 400°C, up to an equivalent strain of  $\sim 8$ . After deformation a homogeneous fine equiaxed duplex microstructure with an average size of 1.1  $\mu\text{m}$  was obtained. Park et al. [17] reported an Al-Cu alloy with ultrafine lamellar eutectic structure exhibited 1.2 GPa strength with obvious plastic strain of  $\sim 2\%$  under compression.

Most Al-Cu alloys (containing 2-4wt% Cu) subjected to SPD show a uniform grain structure and they have an (UTS) of 290-450 MPa and a uniform elongation of 1-4% [18,19]. Tensile properties of an ECAP processed Al-5wt%Cu was referred in [20], in which an UTS of 493 MPa with a low elongation to failure value (less than 10%) was achieved after 8 passes. ECAP processing ( four passes) applied to the Al-4Cu alloy allowed to obtain high (UTS) value about 270 MPa and tensile strain about 8% [21]. An age- hardenable 2219 Al-Cu alloy was severely deformed by multidirectional forging (MDF), followed by solution treatment at T8 aging treatment. The optimal mechanical

properties were obtained when the deformation temperature was 510°C, with UTS of 431 MPa and elongation of 6.5% at room temperature [22]. Additionally, the obtained results indicate, that the KoBo method is most effective in reducing the grain size and rebuilding of initial structure. These microstructural changes significantly influence on the mechanical behavior.

#### 4. Summary

The obtained results lead to the following conclusions:

1. In the microstructure of Al-5Cu and Al-25Cu alloys, the dendrites of  $\alpha$  phase were observed. The interdendritic regions consisted of eutectoid composition ( $\alpha + \text{Al}_2\text{Cu}$  phase). The content of composition ( $\alpha + \text{Al}_2\text{Cu}$  phase) increase with Cu increase.
2. The obtained results showed possibility of KoBo deformation of as-cast alloys. KoBo processing contributed to the refinement of microstructure.
3. KoBo processing is required to improve mechanical properties of alloy. The higher compressive strength of Al-25Cu alloy (340 MPa) compared with Al-5Cu alloy (203 MPa) for  $\lambda = 98$  is caused by the intermetallic phase strengthening.
4. The characteristic feature of Al-25Cu alloy for  $\lambda = 98$  is comparable value of compressive strain with Al-5Cu alloy.
5. Deformed Al-25Cu alloys showed high (UTS): 328MPa and 280 MPa for  $\lambda = 30$  and for  $\lambda = 98$  respectively. The alloys reaching elongations in the range 12-13%.

#### Acknowledgements

This work was performed in Faculty of Materials Engineering and Metallurgy of Silesian University of Technology within the work BK-205/RMO/2019

#### REFERENCES

- [1] B. Adamczyk-Cieślak, J. Zdunek, J. Mizera, Conf. Ser.: Mater. Sci. Eng. **123** 012019 (2016) DOI:10.1088/1757899X/123/1/012019
- [2] E. Khafizova, R. Islamgaliev, Conf. Ser. Mater. Sci. Eng. **63**, (2014) DOI:10.1088/1757-899X/63/1/01208
- [3] M. Cabibbo, Intermet. **6**, 3-9 (2015).
- [4] P. Rambabu, N. Eswara Prasad, V.V. Kutumbarao, K.J.H. Wanhill, Aerosp. Mater. DOI10.1007/978-981-10-2134-3\_2
- [5] G. Mrówka-Nowotnik, J. Achiev. Mater. Manufact. Eng. **30** (1), 35-42 (2008).
- [6] W. Bochniak, Teoretyczne i praktyczne aspekty kształtowania plastycznego metali, Metoda KoBo, Wyd. AGH, Kraków (2009).
- [7] W. Bochniak, A. Korbel, P. Ostachowski, S. Ziółkiewicz, J. Borowski, Obr. Plast. Met. **24** (2), 83-97 (2013).
- [8] Z. Qing, W. Jian, M. Amit, H. Ping, W. Fei, X. Kewei, Mech. Mater. Eng. Fac. Pub. (2017) DOI:10.1038/s41524-0170030-2

- [9] J.T. Kim, S.W. Lee, S.W. Hong, H.J. Park, J.Y. Park, N. Lee, Y. Seo, W.M. Wang, J.M. Park, K.B. Kim, *Mat. and Des.* **92**, 1038-1045 (2016).
- [10] M. Eizadjou, A. Kazemi Talachi, H. Danesh Manesh, H. Shakur Shahabi, K. Janghorban, *Comp. Sci. and Tech.* **68**, 2003-2009 (2008).
- [11] J.M. Park, K.B. Kim, D.H. Kim, N. Mattern R. Li, G. Liu, J. Eckert, *Intermet.* **18**, 1829-1833 (2010).
- [12] J.M. Park, N. Mattern, U. Kuhn, J. Eckert, K.B. Kim, K. Chattopadhyay, D.H. Kim, *J. Mater. Res.* **24** (8), 2605-2609 (2009).
- [13] K. Rodak, A. Urbańczyk-Gucwa, M.B. Jabłońska, *Archiv. Civ. Mech. Eng.* **18** (2), 500-507 (2018).
- [14] K. Rodak, A. Urbańczyk-Gucwa, M. Jabłońska, J. Pawlicki, J. Mizera, *Archiv. Civ. Mech. Eng.* **19** (2), 331-337 (2018).
- [15] M. Zha, Y. Li, R.H. Mathiesen, R. Jorge, H.J. Roven, *Acta Mater.* **84**, 42-54 (2015).
- [16] J. Vang, S. Kang, H. Kim, Z. Horita, *J. of Mater. Sci.* **37**, 5223-5227 (2002).
- [17] J.M. Park, K.B. Kim, D.H. Kim, N. Mattern, R. Li, *Intermetallics* **18**, 1829-33 (2010) .
- [18] D.R. Fang, Z.F. Zhang, S.D. Wu, C.X. Huang, N.Q. Zhao, J.J. Li, *Mater. Sci. Eng. A* **426**, 305-313 (2006).
- [19] E. Prados, V. Soldi, M. Ferrante, *Mater. Sci. Eng. A* **503**, 68-70 (2009).
- [20] H. Jia, R. Bjorge, K. Marthinsen, Y. Li, *J. of Alloys and Com.* **697**, 239-248 (2017).
- [21] E.F. Prados, V.L. Sordi, M. Ferrante, *Mater. Res.* **11**, 199-205 (2008).
- [22] H. He, Y. Yi, S. Huang, Y. Zhang, *Mater. Sci. Eng. A* **712**, 414-423 (2018).